DOI: 10.1002/cphc.200900480

# Homolytic versus Heterolytic Dissociation of Alkalimetal Halides: The Effect of Microsolvation

Sílvia Osuna,[b] Marcel Swart,[b, c] Evert Jan Baerends,[a, d] F. Matthias Bickelhaupt,*[a] and Miquel Solà*[b]

Herein we report density functional calculations of homolytic and heterolytic dissociation energies of the diatomic alkalimetal halides MX (M = Li, Na, K, Rb, and Cs and X = F, Cl, Br, I, and At) and their corresponding microsolvated structures $MX\cdot(H_2O)_n$ ($n = 1$ to 4). Our results show that the homolytic dissociation energy of the $MX\cdot(H_2O)_n$ species increases with the number of water molecules involved in the microsolvated salts. On the other hand, the heterolytic dissociation energy follows exactly the opposite trend. As a result, while for the isolated diatomic alkalimetal halides, homolytic dissociation is always favored over heterolytic dissociation, the latter is preferred for CsF and CsCl already for $n = 2$, and for $n = 4$ it is the preferential mode of dissociation for more than half of the species studied.

## 1. Introduction

It belongs to our everyday experience that table salt is readily dissolved in water. Not only table salt but, in general, salts are easily dissolved in aqueous solution. It was Svante Arrhenius who proposed for the first time in his thesis work that when a crystalline sample of a salt is placed into water, it dissociates readily into its ions.[1] The dissociation of salt in water occurs heterolytically because of the strongly stabilizing interactions between the charged species and the polar solvent.

On the other hand, the homolytic dissociation of isolated gas-phase diatomic alkalimetal halide (MX) molecules is preferred over the heterolytic dissociation by about 10–60 kcal mol$^{-1}$ [2–4] (see Table 1), the exact energy gap depending on the difference between the ionization potential of the alkalimetal and the electron affinity of the halogen ($IP_M - EA_X$). The fact that this gap is always positive in gas-phase diatomic alkalimetal halide molecules was a key factor in the landmark experimental femtosecond study by Ahmed H. Zewail and coworkers on the photodissociation dynamics of NaI.[5] For this species, the ground state at small Na–I distances is ionic (or strongly polar), while at large distances it is covalent (or weakly polar). Consequently, there is a crossing point at about 7 Å (for LiF the crossing occurs earlier at ca. 6 Å[6]) between the electronically coupled diabatic ionic and covalent potential energy surfaces. Photoexcitation from the ionic ground state of NaI to the first covalent excited state results in bound oscillatory motion in the excited state potential. Some of the complexes survive for about 10 oscillations before nonadiabatic transition to the covalent ground state takes place to produce *homolytically* dissociated Na and I atoms. Interestingly, the ionic curve is much more stabilized by the solvent than the covalent one and, consequently, the photodissociation dynamics of alkalimetal halides is greatly influenced by the solvent.[7]

Experience shows that gas-phase diatomic alkalimetal halides dissociate homolytically into atoms while in water the same molecules dissociate heterolytically into ions. One can predict that, as we increase the number of molecules in the alkali halide water clusters, $MX\cdot(H_2O)_n$, there should be a transition in the preference from homolytic to heterolytic dissociation. Let us mention here that a previous study of the $MX\cdot(H_2O)_n$ species with M = Li and Na, X = F and Cl, and $n =$ 1–3, concluded that the dissociation remains very much in favor of the neutral atoms even for the clusters with three water molecules.[8] This result is partially in conflict with a previous study on the $LiCl\cdot(H_2O)_n$ clusters that suggested that 3 to 4 water molecules are enough to stabilize the dissociated ions.[9] On the other hand, since molecular alkalimetal halides exhibit a wide range of chemical bonding from the purely ionic to significant covalent bonding,[3,4] it is likely that this transition from homolytic to heterolytic dissociation depends

[a] *Prof. Dr. E. J. Baerends, Prof. Dr. F. M. Bickelhaupt*
*Department of Theoretical Chemistry*
*and Amsterdam Center for Multiscale Modeling*
*Scheikundig Laboratorium der Vrije Universiteit*
*De Boelelaan 1083, 1081 HV Amsterdam (The Netherlands)*
*Fax: (+31) 20-59-87-629*
*E-mail: FM.Bickelhaupt@few.vu.nl*

[b] *S. Osuna, Dr. M. Swart, Prof. Dr. M. Solà*
*Institut de Química Computacional and Departament de Química*
*Universitat de Girona, Campus Montilivi*
*17071 Girona, Catalonia (Spain)*
*Fax: (+34) 972-41-83-56*
*E-mail: miquel.sola@udg.edu*

[c] *Dr. M. Swart*
*Institució Catalana de Recerca i Estudis Avançats (ICREA)*
*08010 Barcelona (Spain)*

[d] *Prof. Dr. E. J. Baerends*
*Department of Chemistry*
*Pohang University of Science and Technology*
*San 31, Hyojadong, Namgu, Pohang, 790-784 (South Korea)*

Supporting information for this article is available on the WWW under http://dx.doi.org/10.1002/cphc.200900480.

  

**Table 1.** Homolytic and heterolytic bond dissociation energies (in kcal mol$^{-1}$) for the different molecules and methods considered. In this first case, the number of water molecules included is zero. The GGA method BP86 with the TZ2P basis set was used to study all the different systems. In some cases relativistic effects using the ZORA approximation and the solvent effects by means of the COSMO model were considered. The alkali-metal–halide distance is expressed in Å. Experimental values for gas-phase diatomic molecular alkali halides are also given.

| | | BP86 NO ZORA | | | BP86 ZORA | | | EXPERIMENTAL | | | BP86 ZORA COSMO | | |
|---|---|---|---|---|---|---|---|---|---|---|---|---|---|
| | | HOMO | HETERO | dist (M–F) | HOMO | HETERO | dist (M–F) | HOMO[a] | HETERO[b] | dist (M–F)[c] | HOMO | HETERO | dist (M–F) |
| Li | F | 138.9 | 190.9 | 1.578 | 138.8 | 190.9 | 1.578 | 137.5 | 184.1 | 1.56389(5) | 161.9 | −9.4 | 1.656 |
| | | | | | | 186.6[d] | 1.576[d] | | | | | | |
| | Cl | 109.6 | 155.4 | 2.030 | 109.3 | 155.4 | 2.030 | 111.9 | 153.3 | 2.02067(6) | 129.0 | −19.8 | 2.151 |
| | Br | 99.6 | 146.7 | 2.189 | 99.2 | 146.5 | 2.185 | 100.2 | 147.8 | 2.17042(4) | 117.4 | −23.0 | 2.313 |
| | I | 86.8 | 138.0 | 2.419 | 86.4 | 137.9 | 2.399 | 84.6 | 138.7 | 2.39191(4) | 102.2 | −24.3 | 2.541 |
| | At | 81.8 | 135.7 | 2.517 | 78.7 | 134.2 | 2.494 | – | – | – | 93.6 | −25.6 | 2.639 |
| Na | F | 113.5 | 174.0 | 1.948 | 113.2 | 160.3 | 1.947 | 114.0 | 153.9 | 1.92593(6) | 145.9 | −2.2 | 2.062 |
| | | | | | | 156.7[d] | 1.949[d] | | | | | | |
| | Cl | 92.9 | 133.5 | 2.382 | 92.5 | 133.6 | 2.382 | 97.5 | 132.6 | 2.3606(1) | 120.0 | −5.8 | 2.557 |
| | Br | 85.2 | 127.0 | 2.534 | 84.8 | 127.0 | 2.529 | 86.7 | 127.7 | 2.50201(4) | 109.8 | −7.5 | 2.713 |
| | I | 74.8 | 120.8 | 2.748 | 74.3 | 120.7 | 2.732 | 72.7 | 120.3 | 2.71143(4) | 95.3 | −8.0 | 2.927 |
| | At | 70.8 | 119.5 | 2.842 | 67.6 | 118.1 | 2.821 | – | – | – | 87.3 | −8.8 | 3.023 |
| K | F | 120.3 | 160.8 | 2.148 | 119.7 | 147.2 | 2.147 | 117.6 | 139.2 | 2.17144(5) | 150.0 | −1.0 | 2.339 |
| | | | | | | 143.8[d] | 2.163[d] | | | | | | |
| | Cl | 98.5 | 119.2 | 2.652 | 97.9 | 119.3 | 2.650 | 101.3 | 118.0 | 2.6666(1) | 126.3 | −2.3 | 2.903 |
| | Br | 90.8 | 112.7 | 2.819 | 90.1 | 112.7 | 2.811 | 90.9 | 113.6 | 2.82075(5) | 116.6 | −3.5 | 3.077 |
| | I | 80.1 | 106.2 | 3.055 | 79.4 | 106.1 | 3.035 | 76.8 | 106.1 | 3.04781(5) | 102.5 | −3.7 | 3.309 |
| | At | 75.4 | 104.1 | 3.157 | 72.5 | 103.3 | 3.129 | – | – | – | 94.7 | −4.2 | 3.408 |
| Rb | F | 121.5 | 156.9 | 2.262 | 119.6 | 143.3 | 2.262 | 116.1 | 133.6 | 2.26554(5) | 149.5 | −0.5 | 2.480 |
| | | | | | | 139.5[d] | 2.267[d] | | | | | | |
| | Cl | 99.5 | 115.0 | 2.789 | 97.8 | 115.4 | 2.785 | 100.7 | 113.4 | 2.78670(6) | 126.1 | −1.5 | 3.075 |
| | Br | 91.8 | 108.5 | 2.964 | 90.0 | 108.8 | 2.954 | 90.4 | 109.0 | 2.94471(5) | 116.6 | −2.4 | 3.255 |
| | I | 81.3 | 102.2 | 3.207 | 79.5 | 102.5 | 3.183 | 76.7 | 101.9 | 3.17684(5) | 102.6 | −2.6 | 3.491 |
| | At | 77.0 | 100.5 | 3.311 | 72.7 | 99.8 | 3.279 | – | – | – | 94.8 | −3.1 | 3.595 |
| Cs | F | 131.1 | 157.5 | 2.320 | 125.7 | 142.5 | 2.339 | 119.6 | 130.5 | 2.3453(1) | 151.8 | −3.7 | 2.589 |
| | | | | | | 138.8[d] | 2.340[d] | | | | | | |
| | Cl | 106.1 | 112.6 | 2.901 | 101.7 | 112.4 | 2.904 | 106.2 | 112.3 | 2.9062(1) | 128.7 | −4.5 | 3.239 |
| | Br | 98.2 | 105.9 | 3.082 | 93.8 | 105.8 | 3.077 | 96.5 | 108.6 | 3.07221(5) | 119.4 | −5.3 | 3.427 |
| | I | 87.5 | 99.4 | 3.335 | 83.1 | 99.2 | 3.318 | 82.4 | 101.1 | 3.31515(6) | 105.5 | −5.3 | 3.667 |
| | At | 83.5 | 98.1 | 3.443 | 76.3 | 96.5 | 3.417 | – | – | – | 97.8 | −5.7 | 3.777 |

[a] From Tables 8 and 9 of ref. [2]. [b] From Table I of ref. [51]. [c] From Table 2 of ref. [23]. [d] Results obtained with the QZ4P basis set.

on the nature of the chemical bond in MX and of the ions involved.

Thus, the main goal herein is to answer the following two questions: First, how many water molecules are necessary to favor dissociation into ions as compared to dissociation into atoms in alkali halides? And second, how does this number change depending on the nature of the ions involved? To this end, we perform a systematic study of the trends in homolytic and heterolytic dissociation energies across all possible alkalimetal halide salts (with the only exception of francium halides) microsolvated with up to four water molecules. We will focus our attention exclusively to homolytic and heterolytic dissociation energies, that is, the reaction energies of the following two processes, Equation (1):

$$MX \cdot (H_2O)_n \rightarrow M \cdot (H_2O)_m + X \cdot (H_2O)_p \quad (1)$$

and Equation (2):

$$MX \cdot (H_2O)_n \rightarrow M^+ \cdot (H_2O)_m + X^- \cdot (H_2O)_p \quad (2)$$

with M = Li, Na, K, Rb, and Cs; X = F, Cl, Br, I, and At; $n = 0$ to 4; and $m + p = n$. We have restricted our study to four water molecules, because this degree of microsolvation is able to reproduce the change from homolytic to heterolytic dissociation. In addition, increasing the number of water molecules makes the study unfeasible because of the presence of multiple local minima.

Other important properties such as equilibrium geometries, shifts in harmonic frequencies, solvation energies, aggregation energies or the thermodynamic stability of the alkalimetal–halide ion pairs with respect to complete ionic dissociation in clusters [this stability is high even for cluster sizes of $MX\cdot(H_2O)_n$ as large as $n = 50$[10]] are not discussed here. Indeed, many of these properties have been thoroughly analyzed in many theoretical, but also some experimental works on $MX\cdot(H_2O)_n$,[8–17] $M^+\cdot(H_2O)_m$,[18–21] and $X^-\cdot(H_2O)_p$[18,20,22] species (for a review see ref. [23]). To the best of our knowledge, the $M\cdot(H_2O)_m$ and $X\cdot(H_2O)_p$ radical species that are treated herein have not been studied yet. Although we do not discuss the dissociation of alkalimetal halide oligomers or of microcrystal salt fragments,[24,25] the present work is relevant for understanding the microscopic behavior of salts in solution, which is one of the most fundamental issues in chemistry as it is involved in the recognition by ionophores[26] and in diverse biological, environmental, and atmospheric chemical processes.[27] In addition,

  

this work can also be relevant in the solution-phase chemical reactivity field as polar solvent molecules strongly affect the physical and chemical properties of species. Finally, it is worth noting that microsolvation studies such as the present one provide bridges between the gas-phase and condensed-phase chemistries.

## 2. Theoretical Methods

All density functional theory (DFT) calculations were performed with the Amsterdam Density Functional (ADF) program.[28,29] The molecular orbitals (MOs) were expanded in a large uncontracted set of Slater type orbitals (STOs) of triple-ζ quality for all atoms and two sets of polarization functions were included (2p and 3d on H; 3d and 4f on O, F, Cl, Li, Na and K; 4d and 4f on Br, Rb and Cs; 5d and 4f for I and 6d and 5f for At).[30] Moreover, an extra set of p functions has been added to the basis sets of Li (2p), Na (3p), K (4p), Rb (5p) and Cs (6p). The 1s core electrons of oxygen, fluorine, lithium and sodium, the $1s^2$s2p core shells of potassium and chlorine, the 1s2s2p3s3p for rubidium and bromine, the 1s2s2p3s3p4s3d4p for cesium and the 1s2s2p3s3p4s3d4p5s4d for astatine were treated by the frozen-core approximation[29] as it was shown to have a negligible effect on the geometries obtained.[31] From the results of a previous work, we expect that the energetic and geometric results obtained with our TZ2P basis set will not be far from the complete basis set (CBS) limit.[32] An auxiliary set of s, p, d, f, and g STOs was used to fit the molecular density and to represent the Coulomb and exchange potentials accurately for each SCF cycle.

Energies and gradients were computed using the local density approximation (Slater exchange and VWN correlation[33]) with non-local corrections for exchange (Becke88)[34] and correlation (Perdew86)[35] included self-consistently (i.e. the BP86 functional). All open-shell systems were treated with the spin-unrestricted formalism. In some cases, the calculations included scalar relativistic corrections self-consistently using the zeroth-order regular approximation (ZORA).[36] Although it was shown that species such as RbF are not affected by relativistic effects,[37] in others like CsF the relativistic corrections are already significant.[37]

Macroscopic solvent effects were additionally taken into account in some calculations using the COSMO model[38] explicitly both within the solving of the SCF equations and the optimization of the geometry. The solvent radius ($R_s$) for water was taken from experimental data for the macroscopic density ($\rho$) and molecular mass ($M_m$) with the formula $R_s^3 = 2.6752\,M_m/\rho$,[39] leading to a $R_s$ value of 1.9 Å for water; a value of 78.4 was used for the dielectric constant of water. Atomic radii values were taken from the MM3 van der Waals radii,[40] which are available for almost the whole periodic system, and scaled by 0.8333 (the MM3 radii are 20% larger than the normal van der Waals radii due to the specific form for the van der Waals energy within the MM3 force field). Radii of the alkali cations and halide anions were determined such that they reproduce the experimental solvation energy of the ions.[41] The surface charges at the GEPOL93 solvent-excluding surface[42] were corrected for outlying charges. This setup provides a "non-empirical" approach[39] to including solvent effects with a dielectric continuum, and works well for solvation processes.[43]

It is worth mentioning that previously published work on $MX\cdot(H_2O)_n$,[8–17] $M^+\cdot(H_2O)_m$,[18–21] and $X^-\cdot(H_2O)_p$[18,20,22] species already show that several possible H-bonds produce a number of isomers close in energy when we explicitly included several water molecules in the clusters. For the water clusters of all alkalimetal halide salts, alkali cations, and halide anions, we have carefully analyzed all reported structures, looking for the most stable microsolvated isomers. For this reason, although one can never be completely sure, we are quite certain that the structures considered herein are the global minimum structures at the level of theory used. The energies of the global minima in each case have been used to compute the reported dissociation energies corresponding to Equations (1) and (2).

All the geometry optimizations were performed with the QUILD[44] (QUantum-regions Interconnected by Local Descriptions) program, which functions as a wrapper around the ADF program. The QUILD program constructs all input files for ADF, runs ADF, and collects all data; ADF is used only for the generation of the energy and gradients. Furthermore, the QUILD program uses improved geometry optimization techniques, such as adapted delocalized coordinates.[44]

For selected systems, we carried out Møller–Plesset (MP) perturbation theory[45] through the second-order (MP2) approach using Dunning's correlation-consistent polarized valence basis set of triple-ζ quality, that is, cc-pVTZ and also the same basis set augmented with diffuse functions, that is, the aug-cc-pVTZ basis set.[46,47] These MP2 calculations were performed with the Gaussian 03 program.[48] Basis set superposition error (BSSE) corrections were computed for all MP2 dissociation processes using the counterpoise approach as implemented in Gaussian 03.[49]

## 3. Results and Discussion

We divide this section into six subsections, each corresponding to a different number of water molecules solvating the alkalimetal halide water clusters and a final subsection discussing a technical issue.

### 3.1. Isolated Diatomic Alkalimetal Halides

The BP86/TZ2P molecular structures and the homolytic and heterolytic dissociation energies including zero-point energies (ZPE) for alkalimetal fluorides[3] and chlorides[4] were already published by some of us. Table 1 lists the molecular structure and the homolytic and heterolytic bond dissociation energies without ZPE corrections for the different considered diatomic alkalimetal halides and for the different methods analyzed. Figure 1 depicts the molecular structure of all the water clusters of sodium chloride studied herein. The small differences found in the BP86/TZ2P molecular structure of MF and MCl species between our previous studies[3,4] and the present one are due to slight improvements in the basis set and numerical

  

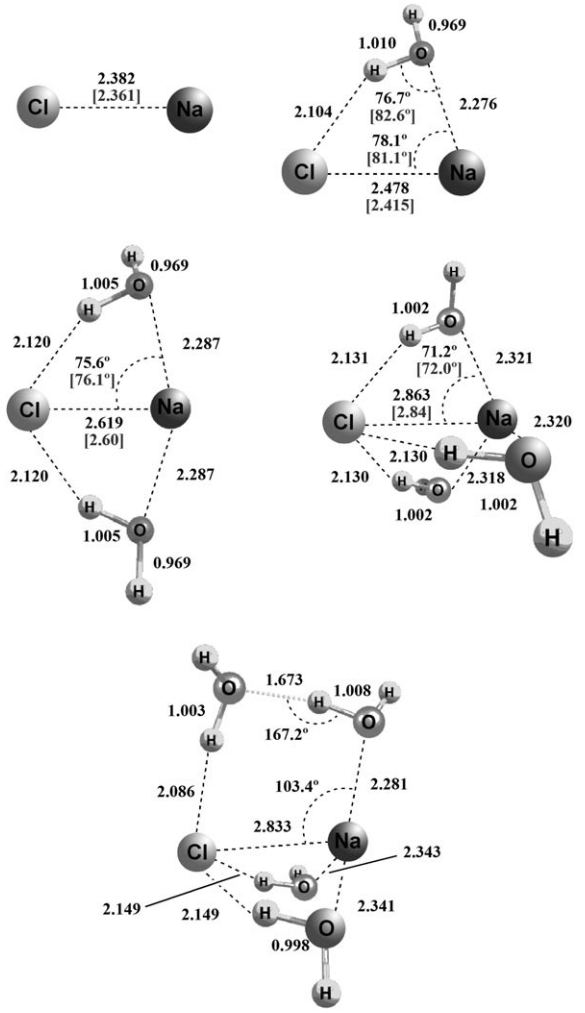


**Figure 1.** Optimized structures in the gas phase at the BP86/TZ2P level, including ZORA for $NaCl\cdot(H_2O)_n$ ($n=0$–4). Most relevant distances and angles are represented in Å and degrees, respectively. Experimental distances and angles are between brackets.

procedures and settings found in the most recent ADF releases.

Let us first discuss the molecular structure of the gas-phase diatomic alkalimetal halides. The results in Table 1 show a good agreement between the experimental and calculated bond lengths of alkalimetal halides, with differences in the 0.01–0.03 Å range. As expected, there is a steady increase in the M–X distance that goes from the 1.578 Å of LiF to the 3.443 Å of CsAt. The influence of the halide in the M–X bond length is more important than that of the metal. Thus, keeping the same metal, a change of X from F to At involves an increase in the bond length of about 0.9–1.1 Å, while with the same halide a change in the metal from Li to Cs involves variations of 0.7–0.9 Å. The increase in the bond length in every step becomes smaller as one descends the periodic table. The relativistic effects are only evident in the M–X bond lengths of the heavier members of the series, that is, MX alkalimetal halides with either M = Rb and Cs and/or X = I and At. In all cases, except for CsF and CsCl, there is a reduction of the M–X distance when including relativistic corrections. In general, relativistic M–X bond lengths are closer to the experimental values (all in the gas-phase) than nonrelativistic distances. Solvent effects computed with the COSMO methodology increase the M–X bond lengths by 0.1–0.3 Å. This agrees with previous studies which have shown that the M–X bond lengthens as the number of water molecules ($n$) increases in the $MX\cdot(H_2O)_n$ cluster.[8,13–15]

The trends in homolytic dissociation energies of MX species ($MX \rightarrow M^{\bullet} + X^{\bullet}$) for a given halide are similar to those found in previous studies.[3,4] For a given halide, there is an important reduction of the homolytic dissociation energy from Li to Na and then it slightly increases from Na to K to Rb and to Cs. This is a somewhat surprising result, as one would expect an increase in the bond strength of ionic bonds if the metal becomes more electropositive, that is, from Li to Cs. The observed trend can be explained by the overlap between the $np_\sigma(X)$ and ns(M) bonding orbitals and the different participation of the $np_\sigma(M)$ in the bonding as discussed by some of us before.[3,4] For a given alkalimetal, the trend is the one expected for ionic bonds, that is, a reduction in the bond strength from F to At. The reduction in the bond strength in every step down group 17 becomes, in general, smaller as one descends the periodic table. The homolytic dissociation energies for the heavier members of the series change significantly (up to 7 kcal mol$^{-1}$ reduction) and become, in general, more similar to the experimental values if relativistic effects are added. It is worth noting that, whereas we find the usual relativistic bond contraction, the relativistic bond energy is, contrary to the commonly observed relativistic stabilization, always reduced for our systems. This is related to the ionic character of the bond at equilibrium geometry. The ionization energy of the metal is relativistically increased, but there is only a minor relativistic effect on the electron affinity of the halogen. The increase in relativistic ionization energy is larger than the relativistic increase of the bond strength between the ions, which is very small. This special circumstance has been noted and analyzed for the heavy metal halide AuCl a long time ago.[50] Differences between experimental and theoretical homolytic dissociation energies of 1 or 2 kcal mol$^{-1}$ are the most frequent, with the largest deviation of 6 kcal mol$^{-1}$ in the case of CsF. Interestingly, the homolytic dissociation energies increase significantly in water solution, as deduced from the COSMO results, by an amount that ranges from 14.9 kcal mol$^{-1}$ (LiAt) up to 32.7 kcal mol$^{-1}$ (NaF). This is the result of diatomic alkalimetal halides being better solvated because of partial charge separation ($M^{\delta+}X^{\delta-}$) than the neutral alkalimetal and halogen radicals.

It is clearly seen in Table 1 that the heterolytic or ionic dissociation ($MX \rightarrow M^{+} + X^{-}$) is generally unfavorable with respect to the homolytic one: in all cases, the heterolytic dissociation energies are 1.1–1.7 times higher (11–61 kcal mol$^{-1}$) than the homolytic ones. This is because charge separation is highly unfavorable in the gas-phase. Interestingly, relativistic corrections are less important in heterolytic than in homolytic dissociation energies. Differences in relativistically corrected or uncorrected heterolytic dissociation energies are always less than 2 kcal mol$^{-1}$. This small relativistic effect has the same origin as the

  

relativistic *decrease* of the bond energy with respect to neutral atoms that we have cited before. The decrease in relativistic bond strength with respect to neutral atoms, which we attributed to the relativistically enhanced cost of formation of the ions in the ionic bond in the first place, is naturally canceled by the increase in the ionization of the neutral atoms to ions, if we take the ions as dissociation products. Equivalently, when we refer the bond energy to the ions, the relativistic increase in the ionization energy of M to $M^+$ has already been taken into account, and there is very little relativistic effect on the bond energy between the ions, which has a large electrostatic component anyway. The trends in heterolytic dissociation energies of MX species are those expected for ionic bonds, that is, they increase when going from the heavier elements (with a more diffuse charge) to the lighter ones (with a more concentrated charge) of the series, that is, from At to F and from Cs to Li. Not only charge concentration but also the shorter bond distance in lighter MX species favors the electrostatic interactions thus increasing the heterolytic dissociation energy. When compared to the experimental results, it is found that, with the exception of alkalimetal fluorides, there is a good agreement between our computed and the experimental heterolytic dissociation energies, the error being in many cases smaller than 1 kcal mol$^{-1}$ and only for CsBr does it become relatively large (2.8 kcal mol$^{-1}$). For the alkalimetal fluorides the difference between experimental and theoretical heterolytic dissociation energies are much bigger (from 6.4 kcal mol$^{-1}$ in NaF to 12.0 kcal mol$^{-1}$ in CsF). A possible source of the error might be that the TZ2P basis set, although relatively flexible, still does not have sufficiently diffuse STOs for describing the very diffuse fluoride anion. To investigate this point, we have recomputed heterolytic dissociation energies for the alkalimetal fluorides using the bigger QZ4P basis set, which provides results close to the CBS limit. Values included in Table 1 show that there is some improvement when going from the TZ2P to the QZ4P in the case of the heterolytic dissociation energies of alkalimetal fluorides, while bond lengths show little influence on the basis set. Although the computed heterolytic dissociation energies are still bigger than the experimental values (from 2.5 kcal mol$^{-1}$ in LiF to 8.3 kcal mol$^{-1}$ in CsF), the errors are smaller with the largest basis set by 2.72 (LiF) and 1.45 (CsF). Further basis set improvement may lead to an additional improvement of the theoretical results. Another possible source of error could be the lack of compact functions in the description of the $Na^+$ to $Cs^+$ cations. Although we have not analyzed this point in detail, it is quite unlikely that cations are not properly described with the TZ2P basis set since, except for the fluorides, computed values of the heterolytic dissociation energies are in excellent agreement with the experimental results. Finally, the possibility that experimental values of the alkalimetal fluorides heterolytic dissociation energies are somewhat underestimated cannot be ruled out. Indeed, the fact that experimental errors were larger for alkalimetal fluorides than for the rest of alkalimetal halides was already put forward by Brumer and Karplus in their work (see footnote [e] of Table I in ref. [51]).

Finally, when the effect of the aqueous solution is taken into account, the heterolytic dissociation becomes a thermoneutral or slightly exothermic process in accordance with the experimental observation of spontaneous salt dissolution in water. It is worth noting that entropy corrections are not included in our calculations but they should also favor dissociation. Other factors, such as the fact that we are considering an isolated alkali metal molecule instead of a rock salt or the approximations done in continuum solvation models[52] can also be not negligible. In particular, there is much work showing that radii parameterization is essential to get good results when using continuum models.[39,53,54] Small changes in radii can produce quite different hydration energies, especially in the case of atomic cations and anions.[39,53] Table 2 compares the experimental[55] and computed Gibbs free energy of solvation of the ions studied. As can be seen, the COSMO method reproduces correctly the experimental trends. The theoretical estimates for the anions conform quite well to the experimental results, while for the alkalimetal cations the theoretical values are underestimated by about 10 kcal mol$^{-1}$.

**Table 2.** Experimental and computed Gibbs free energy of solvation (in kcal mol$^{-1}$) for the different ions considered. The GGA method BP86 was used to study all the different systems, including relativistic effects using the ZORA approximation and the solvent effects by means of the COSMO model.

| | Exp. $\Delta G_{solv}$[a] | COSMO $\Delta G_{solv}$ |
|---|---|---|
| $Li^+$ | −126.5 | −118.7 |
| $Na^+$ | −101.3 | −90.5 |
| $K^+$ | −84.1 | −73.6 |
| $Rb^+$ | −78.7 | −68.8 |
| $Cs^+$ | – | −67.4 |
| $F^-$ | −102.5 | −103.5 |
| $Cl^-$ | −72.7 | −75.4 |
| $Br^-$ | −66.3 | −68.6 |
| $I^-$ | −57.4 | −60.3 |
| $At^-$ | – | −57.0 |

[a] Experimental values from ref. [55].

### 3.2. MX·$H_2O$ Clusters

Given that the results in the previous section indicate that the ZORA values are somewhat better, especially for the heaviest members of the series, from now on we discuss only the values obtained including this correction. Results obtained without the ZORA relativistic approach can be found in the Supporting Information.

As to the molecular structure, the most stable MX·$H_2O$ conformer in all cases is the one depicted in Figure 1 for NaCl·$H_2O$. In this structure the alkalimetal halide and the water molecule form a four-membered ring (4-MR) with the O atom of the water interacting with the alkalimetal and one of the H atoms of water in close contact with the halide. This result is in agreement with previous theoretical and experimental studies.[8,9,11,13–17,24] As can be seen from Figure 1, the computed bond lengths and angles of NaCl·$H_2O$ are close to those determined experimentally by Fourier-transform microwave spec-

  

trometry.[11] Note also the increase by 0.096 (theor.) or 0.091 Å (exp.) in the Na–Cl bond length due to the presence of the interacting water molecule. The increase in the M–X bond distances in the presence of water molecules is a general behavior that has been discussed in detail before[8,13–15,17] and is not analyzed here.

Table 3 lists the homolytic and heterolytic bond dissociation energies derived from Equations (1) and (2) for $n=1$. For each system and reaction, we have computed the two existing possibilities, either $m=1$ and $p=0$ or $m=0$ and $p=1$ and, for each combination ($m$,$p$), we have taken the energetically most favorable structural conformation to derive the values of Table 3. In the case of homolytic dissociation, differences between the two possibilities are small. However, in the case of heterolytic dissociation, the energy difference of having the cation or the anion interacting with the water molecule can be as large as about 20 kcal mol$^{-1}$, as can be deduced from the experimental enthalpies for the hydration reaction $A + H_2O \rightarrow A{\cdot}H_2O$ ($A = Li^+$, −34.0; $Na^+$, −24.0; $K^+$, −17.9; $Rb^+$, −15.9; $Cs^+$, −13.7; $F^-$, −23.3; $Cl^-$, −13.1; $Br^-$, −12.6; $I^-$, −10.2 kcal mol$^{-1}$).[19,20] Our computed electronic monohydration energies deviate by less than 2.2 and 3.1 kcal mol$^{-1}$ for cations and anions, respectively, from these experimental hydration enthalpies. A larger deviation is found in the case of $F^-$, where the experimental value is approximately 12 kcal mol$^{-1}$ higher in energy as compared to theory. The hydration energy for fluoride calculated at BP86 using the larger QZ4P basis set is −32.0 kcal mol$^{-1}$, which is still 8.7 kcal mol$^{-1}$ higher than the experimental value. On the other hand, MP2 calculations using the aug-cc-pVTZ and aug-cc-pVQZ[46,56] basis sets predict hydration energies of −27.6 and −27.5 kcal mol$^{-1}$, respectively. The latter results show that the BP86 functional tends to overestimate the hydration energy for $F^-$ anion somewhat, whereas MP2 gives more accurate hydration energies that are not highly affected by the size of the basis set used (the difference between MP2/aug-cc-pVTZ and MP2/aug-cc-pVQZ is just 0.1 kcal mol$^{-1}$). As expected, solvation is more exothermic for the smallest cations and anions. According to our calculations, $MX{\cdot}H_2O$ with M = Li and Na or X = I and At heterolytically dissociates into $M^+{\cdot}H_2O + X^-$ in all cases except for X = F and CsI. The LiF case is in clear disagreement with experimental monohydration enthalpies of alkalimetal cations and halide anions, but, in general, the results obtained either follow the expected trends or the differences in energetic stabilization due to hydration of $M^+$ and $X^-$ ions are relatively small. In particular, $LiCl{\cdot}H_2O$ dissociates into $Li^+{\cdot}H_2O$ and $Cl^-$ as found previously by Woon and Dunning.[8]

The results in Table 3 show that, for $n=1$, in all cases the homolytic dissociation [Eq. (1)] is still more favorable than the heterolytic one [Eq. (2)]. However, the energy differences between homolytic and heterolytic dissociations are now smaller by about 6 to 25 kcal mol$^{-1}$. Thus, for instance, in the case of isolated LiF, the homolytic dissociation costs 52.1 kcal mol$^{-1}$ less than the heterolytic dissociation, while for $LiF{\cdot}H_2O$ the difference is 41.3 kcal mol$^{-1}$. As before, the smallest difference between homolytic and heterolytic dissociation is found in the case of the CsX species. For the calculations of the $MX{\cdot}H_2O$ species including solvent effects with COSMO, we have also calculated the dissociation energies considering the two existing possibilities ($m=1$ and $p=0$ or $m=0$ and $p=1$) and we have taken the energetically most favorable result. In general, we have the same radical or ionic association with the intervening water molecule as that found when the effect of aqueous solution were not included, but in some cases, especially for the homolytic dissociation, we observe some changes. An increase in the homolytic dissociation energy is observed in all cases when including solvent effects with COSMO for the same reason discussed in isolated MX species. The heterolytic dissociation is slightly exothermic in all species. The values for the het-

**Table 3.** Homolytic and heterolytic bond dissociation (in kcal mol$^{-1}$) for the different considered molecules and methods when one water molecule is included in the process. The GGA method BP86 was used to study all the different systems, including relativistic effects using the ZORA approximation and the solvent effects by means of the COSMO model. The number of water molecules situated close to the alkalimetal (M) followed by the number of water molecules near the halide (X) are also represented.

| | | BP86 ZORA | | | | | | BP86 ZORA COSMO | | | | | |
|---|---|---|---|---|---|---|---|---|---|---|---|---|---|
| | | HOMO | M | X | HETERO | M | X | HOMO | M | X | HETERO | M | X |
| Li | F | 133.7 | 0 | 1 | 175.0 | 0 | 1 | 149.5 | 0 | 1 | −3.2 | 0 | 1 |
| | Cl | 114.8 | 1 | 0 | 141.0 | 1 | 0 | 134.0 | 0 | 1 | −8.0 | 1 | 0 |
| | Br | 104.9 | 1 | 0 | 132.3 | 1 | 0 | 121.7 | 1 | 0 | −10.8 | 1 | 0 |
| | I | 92.4 | 1 | 0 | 123.9 | 1 | 0 | 106.7 | 1 | 0 | −11.7 | 1 | 0 |
| | At | 84.7 | 1 | 0 | 120.3 | 1 | 0 | 97.5 | 1 | 0 | −13.0 | 1 | 0 |
| Na | F | 111.1 | 0 | 1 | 147.3 | 0 | 1 | 126.8 | 0 | 1 | −2.9 | 0 | 1 |
| | Cl | 99.7 | 0 | 1 | 128.4 | 1 | 0 | 117.5 | 0 | 1 | −1.4 | 0 | 1 |
| | Br | 92.9 | 0 | 1 | 120.9 | 1 | 0 | 110.1 | 0 | 1 | −2.9 | 1 | 0 |
| | I | 84.1 | 0 | 1 | 114.0 | 1 | 0 | 99.5 | 0 | 1 | −3.4 | 1 | 0 |
| | At | 77.5 | 1 | 0 | 110.9 | 1 | 0 | 92.4 | 0 | 1 | −4.1 | 1 | 0 |
| K | F | 115.9 | 0 | 1 | 132.5 | 0 | 1 | 131.7 | 0 | 1 | −0.8 | 0 | 1 |
| | Cl | 104.1 | 0 | 1 | 118.8 | 0 | 1 | 120.3 | 0 | 1 | −1.4 | 0 | 1 |
| | Br | 97.4 | 0 | 1 | 111.8 | 1 | 0 | 113.7 | 0 | 1 | −1.8 | 0 | 1 |
| | I | 88.4 | 0 | 1 | 104.6 | 1 | 0 | 103.2 | 0 | 1 | −2.1 | 0 | 1 |
| | At | 81.8 | 1 | 0 | 101.5 | 1 | 0 | 96.7 | 0 | 1 | −2.0 | 1 | 0 |
| Rb | F | 114.9 | 0 | 1 | 127.7 | 0 | 1 | 131.4 | 0 | 1 | −0.1 | 0 | 1 |
| | Cl | 103.4 | 0 | 1 | 114.3 | 0 | 1 | 118.9 | 1 | 0 | −0.9 | 0 | 1 |
| | Br | 96.7 | 0 | 1 | 110.0 | 0 | 1 | 109.0 | 1 | 0 | −1.9 | 0 | 1 |
| | I | 87.9 | 0 | 1 | 102.1 | 1 | 0 | 95.3 | 1 | 0 | −1.6 | 0 | 1 |
| | At | 81.5 | 0 | 1 | 99.1 | 1 | 0 | 87.7 | 1 | 0 | −1.7 | 0 | 1 |
| Cs | F | 118.4 | 0 | 1 | 124.3 | 0 | 1 | 133.2 | 0 | 1 | −3.9 | 0 | 1 |
| | Cl | 106.1 | 0 | 1 | 110.1 | 0 | 1 | 122.4 | 0 | 1 | −4.0 | 0 | 1 |
| | Br | 99.5 | 0 | 1 | 105.8 | 0 | 1 | 115.4 | 0 | 1 | −4.7 | 0 | 1 |
| | I | 90.6 | 0 | 1 | 99.7 | 1 | 0 | 104.5 | 0 | 1 | −5.5 | 0 | 1 |
| | At | 84.4 | 1 | 0 | 99.1 | 0 | 1 | 98.4 | 0 | 1 | −4.8 | 0 | 1 |

  

erolytic dissociation in the M=Li species notably differ from those obtained in isolated LiX systems. For the rest, the values are quite similar, indicating a good behavior of the continuum model. As a general trend, both the homolytic and heterolytic dissociation is easier when going from X=F to At.

### 3.3. $MX\cdot(H_2O)_2$ Clusters

The most stable structure for the $MX\cdot(H_2O)_2$ species in all cases is the one depicted in Figure 1 for $NaCl\cdot(H_2O)_2$. In this structure the alkalimetal halide and the two water molecules form two 4-MRs analogous to that found in the $MX\cdot H_2O$ compounds. This kind of structure was already proposed in previous studies.[8,11,13,15,17,24] Another structure with two water molecules interacting with the MX species and forming a 6-MR bridge is somewhat less stable. The ZORA BP86/TZ2P bond lengths and angles of $NaCl\cdot(H_2O)_2$ shown in Figure 1 are in good agreement with those determined experimentally by Fourier transform microwave spectrometry.[11] Again there is a remarkable increase in the M–X distance with the inclusion of the second water molecule.

Table 4 gathers the homolytic and heterolytic dissociation for the $MX\cdot(H_2O)_2$ species. In this case we have also computed all possibilities for the final water molecules in Equations (1) and (2), namely $m=0$, 1, and 2 with $p=2-m$, and we have always taken the option leading to the lowest total energy. Interestingly, differences in hydration energies between cations and anions due to the interaction with the second water molecule are smaller (although still significant) as can be seen from the experimental enthalpies for the hydration reaction $A\cdot H_2O + H_2O \rightarrow A\cdot(H_2O)_2$ ($A=Li^+$, −25.8; $Na^+$, −19.8; $K^+$, −16.1; $Rb^+$, −13.6; $Cs^+$, −12.5; $F^-$, −16.6; $Cl^-$, −12.7; $Br^-$, −12.3; $I^-$, −9.8 kcal mol$^{-1}$).[19,20] Our theoretical estimates of the electronic energies of these experimental hydration enthalpies deviate by less than 2.3 and 2.0 kcal mol$^{-1}$ for cations and anions, respectively. As it happens with the hydration reaction involving a single water molecule, a larger deviation is found for $F^-$ (the theoretical hydration enthalpy is overestimated by 6 kcal mol$^{-1}$). As can be seen from the values of Table 4, homolytic dissociation is still preferred over heterolytic dissociation, except in one case, the CsF species. In addition, heterolytic dissociation is marginally preferred in the case of CsCl. Not unexpectedly, heterolytic dissociation is favored over homolytic dissociation for those species having heavy alkalimetal atoms with low ionization potentials and light halides with large electron affinities and large solvation energies. The energy differences between homolytic and heterolytic dissociation are less and now range from −1.8 to 28.6 kcal mol$^{-1}$. If the overestimation of our computed heterolytic dissociation energies of the MF species affects the $MF\cdot(H_2O)_2$ species to the same extent, then the heterolytic splitting for KF and RbF would already be favored over the homolytic splitting for $n=2$. As found in the previous section, the inclusion of the continuum solvent effects increases the homolytic dissociation energy and reduces that for heterolytic dissociation. The reduction in the heterolytic dissociation energy is less than that found in isolated MX and $MX\cdot H_2O$ species. In some cases (KCl, RbF, RbCl, and RbBr), the heterolytic dissociation energy becomes slightly positive. In general, there is not a clear trend in the heterolytic dissociation and the process is almost thermoneutral in most cases. As we have emphasized before, there are some approximations (radii parameterization, lack of thermal and entropy corrections…) in these COSMO calculations that may affect the trends observed. In general, the results presented herein that have been obtained in microsolvated systems are likely to be more reliable than those that incorporate macrosolvation effects through the COSMO approach.

**Table 4.** Homolytic and heterolytic bond dissociation (in kcal mol$^{-1}$) for the different considered molecules and methods when two water molecules are included in the process. The GGA method BP86 was used to study all the different systems, including relativistic effects using the ZORA approximation and the solvent effects by means of the COSMO model. The number of water molecules situated close to the alkalimetal (M) followed by the number of water molecules near the halide (X) are also represented.

| | | BP86 ZORA | | | | | | BP86 ZORA COSMO | | | | | |
|---|---|---|---|---|---|---|---|---|---|---|---|---|---|
| | | HOMO | M | X | HETERO | M | X | HOMO | M | X | HETERO | M | X |
| Li | F | 139.0 | 0 | 2 | 162.2 | 1 | 1 | 143.9 | 1 | 1 | −2.5 | 0 | 2 |
| | Cl | 119.0 | 2 | 0 | 130.6 | 2 | 0 | 132.0 | 1 | 1 | −1.4 | 1 | 1 |
| | Br | 108.4 | 2 | 0 | 121.2 | 2 | 0 | 123.2 | 2 | 0 | −3.5 | 2 | 0 |
| | I | 96.2 | 2 | 0 | 113.2 | 2 | 0 | 108.5 | 2 | 0 | −4.2 | 2 | 0 |
| | At | 88.5 | 2 | 0 | 109.5 | 2 | 0 | 100.2 | 2 | 0 | −5.3 | 2 | 0 |
| Na | F | 115.0 | 0 | 2 | 143.6 | 0 | 2 | 124.4 | 0 | 2 | −2.2 | 0 | 2 |
| | Cl | 105.2 | 0 | 2 | 124.4 | 2 | 0 | 115.4 | 0 | 2 | −1.0 | 1 | 1 |
| | Br | 98.3 | 0 | 2 | 116.3 | 2 | 0 | 110.8 | 0 | 2 | 0.0 | 2 | 0 |
| | I | 89.8 | 0 | 2 | 109.0 | 2 | 0 | 99.4 | 0 | 2 | −2.0 | 2 | 0 |
| | At | 83.4 | 0 | 2 | 105.5 | 2 | 0 | 94.0 | 0 | 2 | −1.2 | 2 | 0 |
| K | F | 118.4 | 0 | 2 | 127.3 | 0 | 2 | 129.2 | 0 | 2 | −0.3 | 0 | 2 |
| | Cl | 108.1 | 0 | 2 | 117.0 | 1 | 1 | 119.5 | 0 | 2 | 0.7 | 0 | 2 |
| | Br | 101.3 | 0 | 2 | 111.4 | 1 | 1 | 112.9 | 0 | 2 | 0.0 | 0 | 2 |
| | I | 92.7 | 0 | 2 | 103.9 | 2 | 0 | 103.5 | 0 | 2 | −0.2 | 0 | 2 |
| | At | 86.3 | 0 | 2 | 100.5 | 2 | 0 | 96.9 | 0 | 2 | −0.3 | 0 | 2 |
| Rb | F | 117.0 | 0 | 2 | 122.1 | 0 | 2 | 126.9 | 1 | 1 | 0.8 | 0 | 2 |
| | Cl | 106.9 | 0 | 2 | 113.2 | 0 | 2 | 113.0 | 1 | 1 | 0.7 | 0 | 2 |
| | Br | 100.2 | 0 | 2 | 108.9 | 1 | 1 | 106.1 | 1 | 1 | 0.1 | 0 | 2 |
| | I | 91.6 | 0 | 2 | 102.3 | 2 | 0 | 96.0 | 1 | 1 | −0.2 | 0 | 2 |
| | At | 85.3 | 0 | 2 | 99.0 | 2 | 0 | 89.2 | 1 | 1 | −0.3 | 0 | 2 |
| Cs | F | 119.1 | 0 | 2 | 117.3 | 0 | 2 | 131.1 | 2 | 0 | −2.9 | 0 | 2 |
| | Cl | 108.8 | 0 | 2 | 108.2 | 0 | 2 | 120.4 | 2 | 0 | −3.0 | 0 | 2 |
| | Br | 101.9 | 0 | 2 | 104.7 | 0 | 2 | 113.3 | 2 | 0 | −4.2 | 0 | 2 |
| | I | 93.2 | 0 | 2 | 99.3 | 2 | 0 | 103.8 | 2 | 0 | −4.4 | 0 | 2 |
| | At | 87.2 | 0 | 2 | 96.3 | 2 | 0 | 98.0 | 2 | 0 | −3.9 | 0 | 2 |

  

### 3.4. $MX\cdot(H_2O)_3$ Clusters

The number of possible local minima for the $MX\cdot(H_2O)_n$ species increases rapidly with $n$.[9,13] For $n=3$, the global minima found in all cases except for LiF is the one depicted in Figure 1 for $NaCl\cdot(H_2O)_3$, which has three 4-MRs equivalent to those found in $NaCl\cdot(H_2O)$ and $NaCl\cdot(H_2O)_2$. As can be seen in Figure 1, our ZORA BP86/TZ2P bond lengths and angles for $NaCl\cdot(H_2O)_3$ are not far from those reported from experiment (the ONaCl[14,15,17] angle in this case was extrapolated from the values corresponding to $n=1$ and 2).[11] The structure of the most stable isomer in the case $LiF\cdot(H_2O)_3$ consists of one 4-MR similar to those found in $NaCl\cdot(H_2O)_3$ and a 6-MR water bridge (see Figure 2a). The energy difference between these two almost isoenergetic structures for most $MX\cdot(H_2O)_3$ species is around 1 kcal mol$^{-1}$. Interestingly, when the optimization is performed including the effects of aqueous solution with the COSMO method, the global minimum changes for LiCl and LiBr species and becomes that depicted in Figure 2a. For the calculations of the energies involved in Equations (1) and (2), we have always taken the most stable structure at each level of calculation. Once more there is an increase of about 0.2 Å in the M–X distance with the inclusion of the third water molecule.

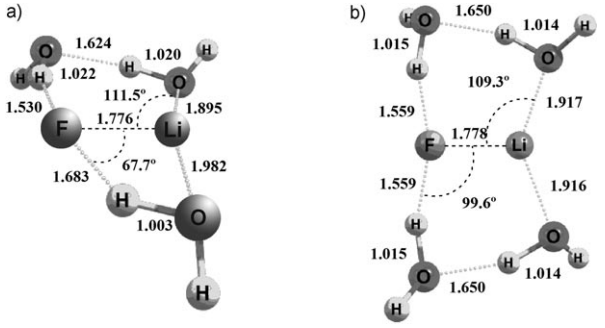


**Figure 2.** Optimized structures in the gas phase at the BP86/TZ2P level, including ZORA for $LiF\cdot(H_2O)_n$ with a) $n=3$ and b) $n=4$. Most relevant distances and angles arerepresented in Å and degrees, respectively.

The homolytic and heterolytic energies of the $MX\cdot(H_2O)_3$ species according to Equations (1) and (2) are gathered in Table 5. In all cases, we have calculated all possible situations for m and p, namely $m=0$ to 3 and $p=3-m$, and we have included in Table 5 the most favorable structural conformation for each combination ($m$,$p$) from an energetic point of view. As can be seen in this table, for all species except CsX (X = F, Cl, and Br) homolytic dissociation is preferred over heterolytic dissociation, although now the differences between these two dissociation processes are relatively small and range from −6.1 (CsF) to 15.8 (NaAt) kcal mol$^{-1}$. The results with the COSMO method show an increase in the homolytic dissociation energy and a reduction of the heterolytic dissociation energy that becomes close to thermoneutral for most cases. At variance with the previous COSMO results, heterolytic dissociation is slightly endothermic with the exception of the $MX\cdot(H_2O)_3$ species with M = Li or Cs and X = Br, I, or At that have slightly exothermic heterolytic dissociations.

### 3.5. $MX\cdot(H_2O)_4$ Clusters

For $n=4$, the global minima found for all $MX\cdot(H_2O)_4$ species except for M = Li is the one depicted in Figure 1 for $NaCl\cdot(H_2O)_4$ that has two 4-MRs equivalent to those found in $NaCl\cdot(H_2O)$ and one 6-MR such as that found in $LiF\cdot(H_2O)_3$. For the $LiX\cdot(H_2O)_4$ species, the most stable structure has two 6-MRs (see Figure 2b for X = F). As can be seen in Figures 1 and 2, there is a small reduction in the Na–Cl bond length when going from $NaCl\cdot(H_2O)_3$ to $NaCl\cdot(H_2O)_4$ while the Li–F bond distance does almost not change when going from $n=3$ to 4. For all species, the two structures (two 4-MRs + one 6-MR vs two

**Table 5.** Homolytic and heterolytic bond dissociation (in kcal mol$^{-1}$) for the different considered molecules and methods when three water molecules are included in the process. The GGA method BP86 was used to study all the different systems, including relativistic effects using the ZORA approximation and the solvent effects by means of the COSMO model. The number of water molecules situated close to the alkalimetal (M) followed by the number of water molecules near the halide (X) are also represented.

| | | BP86 ZORA | | | | | | BP86 ZORA COSMO | | | | | |
|---|---|---|---|---|---|---|---|---|---|---|---|---|---|
| | | HOMO | M | X | HETERO | M | X | HOMO | M | X | HETERO | M | X |
| Li | F | 141.5 | 1 | 2 | 149.8 | 2 | 1 | 145.8 | 1 | 2 | 3.2 | 3 | 0 |
| | Cl | 120.0 | 3 | 0 | 124.7 | 3 | 0 | 129.9 | 2 | 1 | 1.5 | 2 | 1 |
| | Br | 109.9 | 3 | 0 | 115.7 | 3 | 0 | 120.4 | 3 | 0 | −0.3 | 2 | 1 |
| | I | 97.8 | 3 | 0 | 107.9 | 3 | 0 | 104.9 | 3 | 0 | −1.8 | 2 | 1 |
| | At | 90.4 | 3 | 0 | 104.5 | 3 | 0 | 97.6 | 3 | 0 | −1.6 | 2 | 1 |
| Na | F | 125.1 | 1 | 2 | 137.0 | 1 | 2 | 131.9 | 1 | 2 | 2.7 | 3 | 0 |
| | Cl | 108.5 | 0 | 3 | 122.0 | 2 | 1 | 116.9 | 0 | 3 | 3.0 | 2 | 1 |
| | Br | 101.8 | 0 | 3 | 114.1 | 3 | 0 | 111.1 | 0 | 3 | 2.1 | 2 | 1 |
| | I | 93.3 | 0 | 3 | 106.3 | 3 | 0 | 100.3 | 0 | 3 | 1.9 | 2 | 1 |
| | At | 87.1 | 0 | 3 | 102.9 | 3 | 0 | 91.2 | 0 | 3 | 1.9 | 2 | 1 |
| K | F | 120.3 | 0 | 3 | 124.8 | 0 | 3 | 135.0 | 1 | 2 | 2.9 | 3 | 0 |
| | Cl | 110.4 | 0 | 3 | 115.0 | 1 | 2 | 119.5 | 0 | 3 | 3.6 | 1 | 2 |
| | Br | 107.9 | 0 | 3 | 109.9 | 3 | 0 | 111.4 | 0 | 3 | 0.6 | 1 | 2 |
| | I | 95.0 | 0 | 3 | 103.7 | 3 | 0 | 102.8 | 0 | 3 | 2.2 | 1 | 2 |
| | At | 88.7 | 0 | 3 | 100.2 | 3 | 0 | 93.6 | 0 | 3 | 2.2 | 1 | 2 |
| Rb | F | 118.5 | 0 | 3 | 119.3 | 0 | 3 | 124.8 | 1 | 2 | 5.6 | 1 | 2 |
| | Cl | 108.6 | 0 | 3 | 110.3 | 0 | 3 | 112.5 | 1 | 2 | 3.1 | 2 | 1 |
| | Br | 101.9 | 0 | 3 | 107.3 | 0 | 3 | 105.8 | 1 | 2 | 2.2 | 2 | 1 |
| | I | 93.3 | 0 | 3 | 102.8 | 2 | 1 | 95.9 | 1 | 2 | 1.8 | 2 | 1 |
| | At | 87.0 | 0 | 3 | 99.4 | 2 | 1 | 89.4 | 1 | 2 | 1.8 | 2 | 1 |
| Cs | F | 120.0 | 0 | 3 | 113.9 | 0 | 3 | 135.8 | 0 | 3 | 2.7 | 1 | 2 |
| | Cl | 109.9 | 0 | 3 | 104.6 | 0 | 3 | 119.5 | 0 | 3 | 0.3 | 2 | 1 |
| | Br | 103.1 | 0 | 3 | 101.7 | 0 | 3 | 113.6 | 0 | 3 | −0.7 | 2 | 1 |
| | I | 94.5 | 0 | 3 | 98.2 | 0 | 3 | 102.8 | 0 | 3 | −1.0 | 2 | 1 |
| | At | 88.2 | 0 | 3 | 96.6 | 0 | 3 | 93.4 | 0 | 3 | −1.1 | 2 | 1 |

  

6-MRs) are almost isoenergetic. Indeed, when the optimization with the COSMO method is carried out including solvent effects, the most stable structure for all $MX\cdot(H_2O)_4$ systems with the exception of M = K is that of Figure 2b with two 6-MRs. For the calculations of the energies involved in Equations (1) and (2), we have always taken the most stable structure at each level of calculation. To the best of our knowledge there are no experimental structural results for $MX\cdot(H_2O)_4$ species.

Table 6 contains the homolytic and heterolytic bond dissociation energies [Eqs. (1) and (2)] of the $MX(H_2O)_4$ species. We have computed all possible combinations of $p = 0$ to 4 and $m = 4-p$ and, for each of them, we have taken the energetically most favorable structural conformation for both the calculation of the isolated $MX(H_2O)_4$ systems and the same system in water solution using the COSMO model. As can be seen from the values of Tables 1 and 3 to 6, the homolytic dissociation energies of all salts increases when going from $n = 0$ to 4. On the other hand, the dissociation energy relative to $M^+ + X^-$ ions, in general, decreases as more water molecules are included in the model,[8] with some exceptions. This makes the heterolytic dissociation already favorable with respect to the homolytic one for $n = 4$ in thirteen cases: LiX (X = F, Cl, and Br), KX (X = F and Cl), RbX (X = F, Cl, and Br) and CsX. For the rest of the twelve systems, the homolytic dissociation is still preferred but the energetic preference is not larger than 13.0 kcal mol$^{-1}$. Although we have not considered the systems with five water molecules, it is quite likely that for most of the systems the preference of heterolytic over homolytic starts for clusters with $n = 4$ or 5 water molecules. It has to be said that in all cases we are far from reaching spontaneous heterolysis of the salt and, therefore, we are distant from the bulk behavior. Some authors have shown that heterolysis of NaCl into $Na^+$ and $Cl^-$ is not achieved even for $n = 8$.[24] However, for half of the systems analyzed, heterolytic dissociation is already preferred for $n = 4$. Inclusion of solvent effects with the COSMO continuum model, increases marginally the homolytic dissociation and decreases the heterolytic dissociation energy to values that ranges from −0.5 to 8.3 kcal mol$^{-1}$. In most cases, heterolytic dissociation is found to be an endothermic process, but as already mentioned, entropy corrections not included in our results should favor dissociation.

### 3.6. A Final Technical Remark

Some of us and others have shown that two-center three-electron (2c-3e) species, such as for instance the $(H_2O)_2^+$ radical cation,[57] are artificially stabilized by pure DFT methods. On the other hand, correlated ab initio methods such as MP2 do not have this drawback. Since some species, that is, $Cl\cdot H_2O$, that appear in our homolytic dissociation processes are potential 2c-3e systems, we have decided to carry out MP2 calculations on the homolytic and heterolytic dissociation for the simplest system $LiF\cdot(H_2O)_n$, $n = 0$ to 4, to discuss the validity of our DFT results. We expect that the MP2/aug-cc-pVTZ results are not far from being close to the CBS limit.[32] Results obtained with the two basis sets analyzed are collected in Table 7. It is well-known that MP2 calculations present large BSSE corrections especially in conjunction with small basis sets.[58] We therefore computed the alkali metal dissociation energies at the MP2 level including BSSE corrections (see Table 7). As expected, large deviations are found for the case of the smaller cc-pVTZ basis set considered. In fact, the worst results are obtained in the case of the heterolytic dissociation (the maximum error is 23.9 kcal mol$^{-1}$ for $n = 0$), where the use of diffuse functions is critical for the calculation of the $F^-$ energy. The deviations found for the aug-cc-pVTZ basis set are in all cases small (less than 2 kcal mol$^{-1}$). For $n = 0$, we can compare the theoretical estimates with the experimental results (137.5 and 184.1 kcal mol$^{-1}$ for homolytic and heterolytic dissociations). Comparison shows that both the MP2 and DFT (Table 1) results are close to the experimen-

**Table 6.** Homolytic and heterolytic bond dissociation (in kcal mol$^{-1}$) for the different considered molecules when four water molecules are included in the process. The GGA method BP86 was used to study all the different systems, including relativistic effects using the ZORA approximation and the solvent effects by means of the COSMO model. The number of water molecules situated close to the alkalimetal (M) followed by the number of water molecules near the halide (X) are also represented.

| | | BP86 ZORA | | | | | | BP86 ZORA COSMO | | | | | |
|---|---|---|---|---|---|---|---|---|---|---|---|---|---|
| | | HOMO | M | X | HETERO | M | X | HOMO | M | X | HETERO | M | X |
| Li | F | 144.9 | 2 | 2 | 143.6 | 2 | 2 | 145.9 | 3 | 1 | 7.0 | 0 | 4 |
| | Cl | 125.1 | 3 | 1 | 122.6 | 3 | 1 | 127.7 | 3 | 1 | 5.5 | 2 | 2 |
| | Br | 116.1 | 3 | 1 | 114.7 | 4 | 0 | 119.7 | 3 | 1 | 3.8 | 2 | 2 |
| | I | 105.1 | 3 | 1 | 105.7 | 4 | 0 | 109.3 | 3 | 1 | -0.2 | 0 | 4 |
| | At | 100.6 | 3 | 1 | 104.4 | 4 | 0 | 102.5 | 3 | 1 | 2.3 | 0 | 4 |
| Na | F | 128.1 | 1 | 3 | 132.7 | 2 | 2 | 137.3 | 2 | 2 | 7.5 | 0 | 4 |
| | Cl | 113.7 | 0 | 4 | 119.2 | 3 | 1 | 120.2 | 0 | 4 | 8.3 | 2 | 2 |
| | Br | 106.5 | 0 | 4 | 113.2 | 3 | 1 | 113.0 | 0 | 4 | 3.5 | 4 | 0 |
| | I | 97.7 | 0 | 4 | 106.3 | 4 | 0 | 103.6 | 0 | 4 | 3.1 | 0 | 4 |
| | At | 92.0 | 0 | 4 | 105.0 | 4 | 0 | 96.9 | 0 | 4 | 8.3 | 0 | 4 |
| K | F | 127.6 | 0 | 4 | 123.2 | 0 | 4 | 130.4 | 0 | 4 | 4.7 | 0 | 4 |
| | Cl | 114.0 | 0 | 4 | 111.1 | 1 | 3 | 119.9 | 0 | 4 | 5.2 | 4 | 0 |
| | Br | 107.0 | 0 | 4 | 107.8 | 1 | 3 | 113.4 | 0 | 4 | 3.6 | 4 | 0 |
| | I | 98.5 | 0 | 4 | 102.9 | 4 | 0 | 102.8 | 0 | 4 | -0.5 | 0 | 4 |
| | At | 92.6 | 0 | 4 | 101.4 | 4 | 0 | 93.3 | 0 | 4 | 1.9 | 0 | 4 |
| Rb | F | 124.7 | 1 | 3 | 117.0 | 0 | 4 | 131.1 | 0 | 4 | 6.3 | 0 | 4 |
| | Cl | 113.0 | 0 | 4 | 106.8 | 1 | 3 | 115.1 | 1 | 3 | 7.6 | 4 | 0 |
| | Br | 106.0 | 0 | 4 | 103.5 | 1 | 3 | 108.9 | 1 | 3 | 5.9 | 4 | 0 |
| | I | 97.5 | 0 | 4 | 99.8 | 4 | 0 | 99.0 | 1 | 3 | 3.2 | 0 | 4 |
| | At | 91.8 | 0 | 4 | 98.6 | 4 | 0 | 86.2 | 1 | 3 | 2.1 | 0 | 4 |
| Cs | F | 130.1 | 0 | 4 | 111.5 | 0 | 4 | 134.5 | 0 | 4 | 4.1 | 0 | 4 |
| | Cl | 116.2 | 0 | 4 | 102.1 | 0 | 4 | 125.0 | 0 | 4 | 6.3 | 4 | 0 |
| | Br | 109.3 | 0 | 4 | 99.0 | 0 | 4 | 118.5 | 0 | 4 | 4.8 | 4 | 0 |
| | I | 100.8 | 0 | 4 | 95.5 | 0 | 4 | 109.2 | 0 | 4 | 1.4 | 0 | 4 |
| | At | 95.0 | 0 | 4 | 94.0 | 0 | 4 | 102.8 | 0 | 4 | 6.8 | 0 | 4 |

  

**Table 7.** Homolytic and heterolytic bond dissociation (in kcal mol$^{-1}$) for LiF when n water molecules are included ($n$ = 0-4). All the optimizations were performed at the MP2 level of theory using two different basis sets. Basis set superposition error (BSSE) was also considered. The number of water molecules situated close to the alkalimetal (M) followed by the number of water molecules near the halide (X) are also given.

| | MP2/cc-pVTZ | | | | | | MP2/aug-cc-pVTZ | | | | | |
|---|---|---|---|---|---|---|---|---|---|---|---|---|
| n | HOMO | M | X | HETERO | M | X | HOMO | M | X | HETERO | M | X |
| 0 | 138.7 | 0 | 0 | 206.6 | 0 | 0 | 145.7 | 0 | 0 | 180.7 | 0 | 0 |
| 1 | 138.5 | 0 | 1 | 190.3 | 0 | 1 | 138.5 | 0 | 1 | 167.0 | 1 | 0 |
| 2 | 147.8 | 1 | 1 | 176.6 | 1 | 1 | 148.1 | 1 | 1 | 158.4 | 2 | 0 |
| 3 | 153.3 | 2 | 1 | 163.9 | 2 | 1 | 153.1 | 3 | 0 | 147.8 | 2 | 1 |
| 4 | 157.3 | 3 | 1 | 155.3 | 2 | 2 | 157.1 | 3 | 1 | 142.2 | 3 | 1 |
| | MP2/cc-pVTZ BSSE corrected | | | | | | MP2/aug-cc-pVTZ BSSE corrected | | | | | |
| n | HOMO | M | X | HETERO | M | X | HOMO | M | X | HETERO | M | X |
| 0 | 137.0 | 0 | 0 | 182.7 | 0 | 0 | 145.2 | 0 | 0 | 180.1 | 0 | 0 |
| 1 | 134.0 | 0 | 1 | 172.4 | 0 | 1 | 137.8 | 0 | 1 | 165.9 | 1 | 0 |
| 2 | 137.9 | 1 | 1 | 159.4 | 1 | 1 | 146.7 | 1 | 1 | 156.9 | 2 | 0 |
| 3 | 148.5 | 2 | 1 | 146.1 | 2 | 1 | 151.5 | 2 | 1 | 146.2 | 2 | 1 |
| 4 | 152.3 | 3 | 1 | 140.5 | 2 | 2 | 155.2 | 3 | 1 | 140.2 | 3 | 1 |

tal ones, except in the case of the heterolytic dissociation computed at the MP2/cc-pVTZ level that has an error larger than 20 kcal mol$^{-1}$. However, the latter large deviation found is dramatically reduced once BSSE corrections are included, the difference between BSSE-corrected MP2/cc-pVTZ dissociation energy and the experimental value being only of 1.4 kcal mol$^{-1}$. BSSE-corrected MP2/cc-pVTZ heterolytic dissociations are clearly improved when compared to experimental values (when available) or ZORA BP86/TZ2P results. It is worth noting that the values of $p$ and $m$ in Equations (1) and (2) can differ at the MP2 and ZORA BP86/TZ2P levels of theory but overall the differences between BSSE-corrected MP2/aug-cc-pVTZ and ZORA BP86/TZ2P heterolytic dissociation energies are relatively small (from 3.4 ($n$ = 4) to 10.8 ($n$ = 0) kcal mol$^{-1}$). Interestingly, if we take as a reference the BSSE-corrected MP2/aug-cc-pVTZ values, then the ZORA BP86/TZ2P heterolytic dissociation energies are somewhat overestimated. The values that could be more affected by the 2c-3e problem of DFT methods are those corresponding to the homolytic dissociation for the species with $n$ = 1 to 4. In this case, we observe that DFT homolytic dissociations are 4.1 ($n$ = 1) to 10.3 ($n$ = 4) kcal mol$^{-1}$ lower than those obtained with the MP2/aug-cc-pVTZ method because of the spurious stabilization of 2c-3e radical species [M··$(H_2O)_n$ and X·$(H_2O)_n$]. Therefore, our ZORA BP86/TZ2P calculations tend to underestimate homolytic dissociation energies and likely to overestimate somewhat the heterolytic ones. Although the errors are not negligible, the trends remain the same. Indeed, correction of the errors in our dissociation energies will even reinforce the main conclusion reached herein, namely that heterolytic dissociation is favored with respect to homolytic dissociation for $n \geq 4$.

## 4. Conclusions

We have computed the homolytic and heterolytic dissociations of alkali metal halide water clusters, MX·$(H_2O)_n$ ($n$ = 1–4), at the BP86/TZ2P level, including relativistic corrections with the ZORA approach. We have seen that for the isolated gas-phase MX species, homolytic dissociation is favored over the heterolytic dissociation by a factor $BDE_{hetero}/BDE_{homo}$ ranging from 1.1 to 1.7. Our results clearly indicate that the homolytic dissociation energy increases with the number of water molecules present in the cluster, while the heterolytic dissociation energy presents exactly the opposite trend. As a consequence, the energy difference between homolytic and heterolytic dissociations decreases when $n$ increases. As a matter of fact, heterolytic dissociation is already preferred for CsF and CsCl already for $n$ = 2, and for $n$ = 4 it is the preferential mode of dissociation for more than half of the species studied. Interestingly, heterolytic dissociation is found to be a thermoneutral or slightly endothermic process when solvent effects are included using the COSMO approach on top of microsolvated alkalimetal halides.

## Acknowledgements

*We thank the following organizations for financial support: the HPC-Europa program of the European Union, the Netherlands Organization for Scientific Research (NWO), the Ministerio de Ciencia e Innovación (MICINN, project number CTQ2008-03077/BQU), the DIUE of the Generalitat de Catalunya (project number 2009SGR637), the pre-doctoral fellowship (MICINN, project number AP2005-2992) and the National Research School Combination—Catalysis (NRSC-C). This research was also supported by WCU program through the Korea Science and Engineering Foundation (KOSEF: R32-2008-000-10180-0). Excellent service by the Stichting Academisch Rekencentrum Amsterdam (SARA) and the Barcelona Supercomputing Center—Centro Nacional de Supercomputación (BSC-CNS) is gratefully acknowledged.*

**Keywords:** ab initio calculations · alkali metals · density functional calculations · halides · solvent effects

[1] S. Arrhenius, *Z. Phys. Chem.* **1887**, *1*, 631–648.
[2] L. Brewer, E. Brackett, *Chem. Rev.* **1961**, *61*, 425–432.
[3] F. M. Bickelhaupt, M. Solà, C. Fonseca Guerra, *J. Comput. Chem.* **2007**, *28*, 238–250.
[4] F. M. Bickelhaupt, M. Solà, C. Fonseca Guerra, *Inorg. Chem.* **2007**, *46*, 5411–5418.
[5] T. S. Rose, M. J. Rosker, A. H. Zewail, *J. Chem. Phys.* **1988**, *88*, 6672–6673; T. S. Rose, M. J. Rosker, A. H. Zewail, *J. Chem. Phys.* **1989**, *91*, 7415–7436; A. H. Zewail, *J. Phys. Chem. A* **1993**, 97, 12427–12446; A. H. Zewail, *J. Phys. Chem. A* **2000**, *104*, 5660–5694.
[6] M. Hanrath, *Mol. Phys.* **2008**, *106*, 1949–1957.
[7] G. H. Peslherbe, R. Bianco, J. T. Hynes, B. M. Ladanyi, *J. Chem. Soc. Faraday Trans.* **1997**, *93*, 977–988.
[8] D. E. Woon, T. H. Dunning, Jr., *J. Am. Chem. Soc.* **1995**, *117*, 1090–1097.
[9] D. E. Bacelo, Y. Ishikawa, *Chem. Phys. Lett.* **2000**, *319*, 679–686.

  

[10] G. H. Peslherbe, B. M. Ladanyi, J. T. Hynes, *J. Phys. Chem. A* **2000**, *104*, 4533–4548.
[11] A. Mizoguchi, Y. Ohshima, Y. Endo, *J. Am. Chem. Soc.* **2003**, *125*, 1716–1717.
[12] G. H. Peslherbe, B. M. Ladanyi, J. T. Hynes, *J. Phys. Chem. A* **1998**, *102*, 4100–4110; G. H. Peslherbe, B. M. Ladanyi, J. T. Hynes, *Chem. Phys.* **2000**, *258*, 201–224; S. S. M. C. Godinho, P. Cabral do Couto, B. J. Costa Cabral, *J. Chem. Phys.* **2005**, *122*, 044316; C. D. Wick, *J. Phys. Chem. C* **2009**, *113*, 2497–2502.
[13] C. P. Petersen, M. S. Gordon, *J. Phys. Chem. A* **1999**, *103*, 4162–4166.
[14] D. M. Upadhyay, P. C. Mistra, *J. Comput. Chem.* **2003**, *24*, 1336–1347.
[15] A. C. Olleta, H. M. Lee, K. S. Kim, *J. Chem. Phys.* **2006**, *124*, 024321; A. C. Olleta, H. M. Lee, K. S. Kim, *J. Chem. Phys.* **2007**, *126*, 144311.
[16] S. S. M. C. Godinho, P. Cabral do Couto, B. J. Costa Cabral, *Chem. Phys. Lett.* **2004**, *399*, 200–205.
[17] N. J. Singh, H.-B. Yi, S. K. Min, M. Park, K. S. Kim, *J. Phys. Chem. B* **2006**, *110*, 3808–3815.
[18] C. Krekeler, B. Hess, L. Delle Site, *J. Chem. Phys.* **2006**, *125*, 054305; R. Mancinelli, A. Botti, F. Bruni, M. A. Ricci, A. K. Soper, *J. Phys. Chem. B* **2007**, *111*, 13570–13577; J. Enderby, *Chem. Soc. Rev.* **1995**, *24*, 159–168; H. Ohtaki, N. Fukushima, *J. Solution Chem.* **1992**, *21*, 23–38.
[19] I. Džidić, P. Kebarle, *J. Phys. Chem.* **1970**, *74*, 1466–1474.
[20] M. Arshadi, R. Yamdagni, P. Kebarle, *J. Phys. Chem.* **1970**, *74*, 1475–1482.
[21] E. D. Glendening, D. Feller, *J. Phys. Chem.* **1995**, *99*, 3060–3067; H. Dong, W. Liu, D. J. Doren, R. H. Wood, *J. Phys. Chem. B* **2008**, *112*, 13552–13560; J. S. Rao, T. C. Dinadayalane, J. Leszczynski, G. N. Sastry, *J. Phys. Chem. A* **2008**, *112*, 12944–12953; S. Ansell, A. C. Barnes, P. E. Mason, G. W. Neilson, S. Ramos, *Biophys. Chem.* **2006**, *124*, 171–179.
[22] S. Chowdhuri, A. Chandra, *J. Phys. Chem. B* **2006**, *110*, 9674–9680; J. M. Heuft, E. J. Meijer, *J. Chem. Phys.* **2005**, *123*, 094506.
[23] C. Dedonder-Lardeux, G. Grégoire, C. Jouvet, S. Martrenchard, D. Solgadi, *Chem. Rev.* **2000**, *100*, 4023–4038.
[24] S. Yamabe, H. Kouno, K. Matsumura, *J. Phys. Chem. B* **2000**, *104*, 10242–10252.
[25] C. K. Kim, J. Won, H. S. Kim, Y. S. Kang, H. G. Li, C. K. Kim, *J. Comput. Chem.* **2001**, *22*, 827–834; A. Aguado, A. Ayuela, J. M. López, J. A. Alonso, *Phys. Rev. B* **1997**, *56*, 15353–15360; R. N. Barnett, V. Landman, *J. Phys. Chem.* **1996**, *100*, 13950–13958; J. Lai, X. Lu, L. Zheng, *PhysChemComm* **2002**, *5*, 82–87; A. Ayuela, J. M. López, J. A. Alonso, V. Luaña, *Physica B* **1995**, *212*, 329–342; N. G. Phillips, C. W. S. Conover, L. A. Bloomfield, *J. Chem. Phys.* **1991**, *94*, 4980–4987.
[26] J. Yoon, S. K. Kim, N. J. Singh, K. S. Kim, *Chem. Soc. Rev.* **2006**, *35*, 355–360.
[27] A. H. Tang, G. S. Zhuang, Y. Wang, H. Yuan, Y. L. Sun, *Atmos. Environ.* **2005**, *39*, 3397–3406; K. W. Oum, M. J. Lakin, D. O. DeHaan, T. Brauers, B. J. Finlayson-Pitts, *Science* **1998**, *279*, 74–76.
[28] E. J. Baerends, J. Autschbach, A. Bérces, F. M. Bickelhaupt, C. Bo, P. L. de Boeij, P. M. Boerrigter, L. Cavallo, D. P. Chong, L. Deng, R. M. Dickson, D. E. Ellis, L. Fan, T. H. Fischer, C. Fonseca Guerra, S. J. A. van Gisbergen, J. A. Groeneveld, O. V. Gritsenko, M. Grüning, F. E. Harris, P. van den Hoek, C. R. Jacob, H. Jacobsen, L. Jensen, G. van Kessel, F. Kootstra, E. van Lenthe, D. A. McCormack, A. Michalak, J. Neugebauer, V. P. Osinga, S. Patchkovskii, P. H. T. Philipsen, D. Post, C. C. Pye, W. Ravenek, P. Ros, P. R. T. Schipper, G. Schreckenbach, J. G. Snijders, M. Solà, M. Swart, D. Swerhone, G. te Velde, P. Vernooijs, L. Versluis, L. Visscher, O. Visser, F. Wang, T. A. Wesolowski, E. van Wezenbeek, G. Wiesenekker, S. K. Wolff, T. K. Woo, A. L. Yakovlev, T. Ziegler, *ADF2007.01*, SCM, Amsterdam, **2007**.
[29] G. te Velde, F. M. Bickelhaupt, E. J. Baerends, C. Fonseca Guerra, S. J. A. van Gisbergen, J. G. Snijders, T. Ziegler, *J. Comput. Chem.* **2001**, *22*, 931–967.
[30] J. G. Snijders, P. Vernooijs, E. J. Baerends, *At. Data Nucl. Data Tables* **1981**, *26*, 483–509.
[31] M. Swart, J. G. Snijders, *Theor. Chem. Acc.* **2003**, *110*, 34–41.
[32] A. Mintz, A. K. Wilson, P. S. Bagus, *Chem. Phys. Lett.* **2009**, *468*, 286–289.
[33] S. H. Vosko, L. Wilk, M. Nusair, *Can. J. Phys.* **1980**, *58*, 1200–1211.
[34] A. D. Becke, *Phys. Rev. A* **1988**, *38*, 3098–3100.
[35] J. P. Perdew, *Phys. Rev. B* **1986**, *33*, 8800–8802.
[36] E. van Lenthe, E. J. Baerends, J. G. Snijders, *J. Chem. Phys.* **1993**, *99*, 4597–4610.
[37] I. Miadoková, V. Kellö, A. J. Sadlej, *Mol. Phys.* **1999**, *96*, 179–187.
[38] A. Klamt, G. Schüürmann, *J. Chem. Soc. Perkin Trans. 2* **1993**, 799–805; C. C. Pye, T. Ziegler, *Theor. Chem. Acc.* **1999**, *101*, 396–408.
[39] M. Swart, E. Rösler, F. M. Bickelhaupt, *Eur. J. Inorg. Chem.* **2007**, 3646–3654.
[40] N. L. Allinger, X. Zhou, J. Bergsma, *J. Mol. Struct. (Theochem).* **1994**, *312*, 69–83.
[41] R. Gomer, G. Tryson, *J. Chem. Phys.* **1977**, *66*, 4413–4424; T. van der Wijst, C. Fonseca Guerra, M. Swart, F. M. Bickelhaupt, B. Lippert, *Angew. Chem.* **2009**, *121*, 3335–3337; *Angew. Chem. Int. Ed.* **2009**, *48*, 3285–3287.
[42] J. L. Pascual-Ahuir, E. Silla, *J. Comput. Chem.* **1990**, *11*, 1047–1060; J. L. Pascual-Ahuir, E. Silla, I. Tuñón, *J. Comput. Chem.* **1994**, *15*, 1127–1138; E. Silla, I. Tuñón, J. L. Pascual-Ahuir, *J. Comput. Chem.* **1991**, *12*, 1077–1088.
[43] R. S. Bon, B. van Vliet, N. E. Sprenkels, R. F. Schmitz, F. J. J. de Kanter, C. V. Stevens, M. Swart, F. M. Bickelhaupt, M. B. Groen, R. V. A. Orru, *J. Org. Chem.* **2005**, *70*, 3542–3553.
[44] M. Swart, F. M. Bickelhaupt, *Int. J. Quantum Chem.* **2006**, *106*, 2536–2544; M. Swart, F. M. Bickelhaupt, *J. Comput. Chem.* **2008**, *29*, 724–734.
[45] C. Møller, M. S. Plesset, *Phys. Rev.* **1934**, *46*, 618–622.
[46] T. H. Dunning, Jr., *J. Chem. Phys.* **1989**, *90*, 1007–1023.
[47] T. H. Dunning, Jr., K. A. Peterson, A. K. Wilson, *J. Chem. Phys.* **2001**, *114*, 9244–9253; R. A. Kendall, T. H. Dunning, Jr., R. J. Harrison, *J. Chem. Phys.* **1992**, *96*, 6796–6806.
[48] M. J. Frisch, G. W. Trucks, H. B. Schlegel, G. E. Scuseria, M. A. Robb, J. R. Cheeseman, J. A. Montgomery Jr., T. Vreven, K. N. Kudin, J. C. Burant, J. M. Millam, S. S. Iyengar, J. Tomasi, V. Barone, B. Mennucci, M. Cossi, G. Scalmani, N. Rega, G. A. Petersson, H. Nakatsuji, M. Hada, M. Ehara, K. Toyota, R. Fukuda, J. Hasegawa, M. Ishida, T. Nakajima, Y. Honda, O. Kitao, H. Nakai, M. Klene, X. Li, J. E. Knox, H. P. Hratchian, J. B. Cross, V. Bakken, C. Adamo, J. Jaramillo, R. Gomperts, R. E. Stratmann, O. Yazyev, A. J. Austin, R. Cammi, C. Pomelli, J. W. Ochterski, P. Y. Ayala, K. Morokuma, G. A. Voth, P. Salvador, J. J. Dannenberg, G. Zakrzewski, S. Dapprich, A. D. Daniels, M. C. Strain, O. Farkas, D. K. Malick, A. D. Rabuck, K. Raghavachari, J. B. Foresman, J. V. Ortiz, Q. Cui, A. G. Baboul, S. Clifford, J. Cioslowski, B. B. Stefanov, G. Liu, A. Liashenko, P. Piskorz, I. Komaromi, R. L. Martin, D. J. Fox, T. Keith, M. A. Al-Laham, C. Y. Peng, A. Nanayakkara, M. Challacombe, P. M. W. Gill, B. Johnson, W. Chen, M. W. Wong, C. Gonzalez, J. A. Pople *Gaussian 03, Version C.02*, Gaussian, Inc., Pittsburgh, PA, **2003**.
[49] S. F. Boys, F. Bernardi, *Mol. Phys.* **1970**, *19*, 553–566.
[50] T. Ziegler, E. J. Snijders, E. J. Baerends, *J. Chem. Phys.* **1981**, *74*, 1271–1284.
[51] P. Brumer, M. Karplus, *J. Chem. Phys.* **1973**, *58*, 3903–3918.
[52] D. Laria, R. Fernández-Prini, *J. Chem. Phys.* **1995**, *102*, 7664–7673.
[53] A. Nicholls, S. Wlodek, J. A. Grant, *J. Phys. Chem. B* **2009**, *113*, 4521–4532.
[54] M. Orozco, F. J. Luque, *Chem. Phys.* **1994**, *182*, 237–248; A. H. De Vries, P. T. van Duijnen, A. H. Juffer, *Int. J. Quantum Chem.* **1993**, *48*, 451–466; C. J. Cramer, D. G. Truhlar, *Chem. Rev.* **1999**, *99*, 2161–2200.
[55] M. D. Tissandier, K. A. Cowen, W. Y. Feng, E. Gundlach, M. H. Cohen, A. D. Earhart, J. V. Coe, T. R. Tuttle, Jr., *J. Phys. Chem. A* **1998**, *102*, 7787–7794.
[56] D. E. Woon, T. H. Dunning, Jr., *J. Chem. Phys.* **1993**, *98*, 1358–1371.
[57] M. Sodupe, J. Bertran, L. Rodríguez-Santiago, E. J. Baerends, *J. Phys. Chem. A* **1999**, *103*, 166–170; H. Chermette, I. Ciofini, F. Mariotti, C. Daul, *J. Chem. Phys.* **2001**, *115*, 11068–11079; F. M. Bickelhaupt, A. Diefenbach, S. P. de Visser, L. J. de Koning, N. M. M. Nibbering, *J. Phys. Chem. A* **1998**, *102*, 9549–9553; T. Bally, G. N. Sastry, *J. Phys. Chem. A* **1997**, *101*, 7923–7925; F. M. Bickelhaupt, E. J. Baerends in *Review in Computational Chemistry, Vol. 15* (Eds.: K. B. Lipkowitz, D. B. Boyd), Wiley-VCH, New York, **2000**, pp. 1–86; B. Braïda, P. C. Hiberty, A. Savin, *J. Phys. Chem. A* **1998**, *102*, 7872–7877.
[58] G. T. de Jong, M. Solà, L. Visscher, F. M. Bickelhaupt, *J. Chem. Phys.* **2004**, *121*, 9982–9992.


Received: June 23, 2009
Revised: August 12, 2008
Published online on September 18, 2009

  